Universiteit
Leiden
The Netherlands

Bacterial heterozygosity promotes survival under multidrug selection

Shitut, S.S.; Dijk, T. van; Claessen, D.; Rozen, D.E.

Citation
Shitut, S. S., Dijk, T. van, Claessen, D., & Rozen, D. E. (2025). Bacterial heterozygosity promotes survival under multidrug selection. *Current Biology, 35*(7), 1437-1445.E3. doi:10.1016/j.cub.2025.02.012

Version:	Publisher's Version
License:	Creative Commons CC BY 4.0 license
Downloaded from:	https://hdl.handle.net/1887/4287686

Note: To cite this publication please use the final published version (if applicable).

Article

Current Biology

Bacterial heterozygosity promotes survival under multidrug selection

Graphical abstract

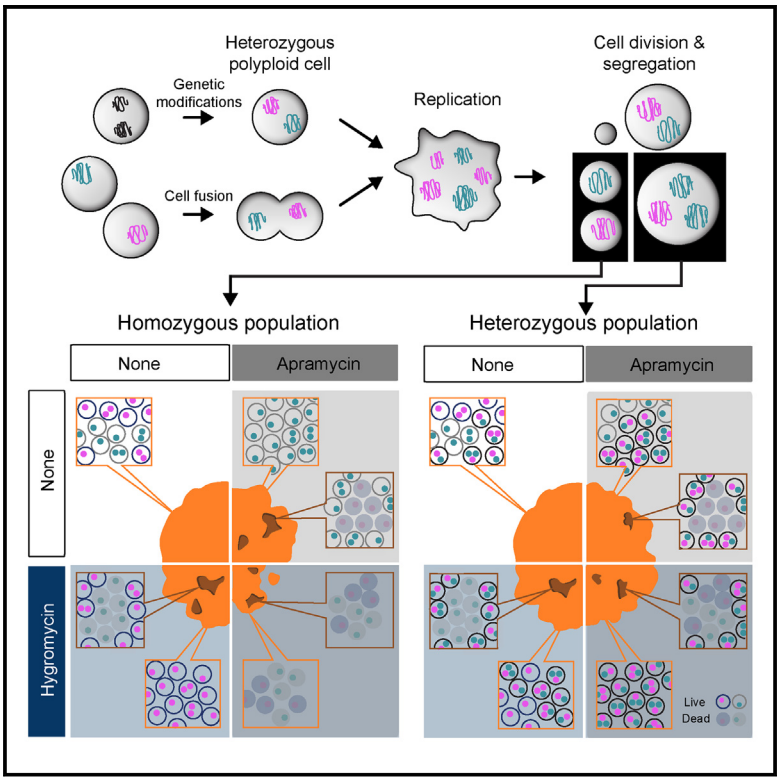

Authors

Shraddha Shitut, Thomas van Dijk, Dennis Claessen, Daniel Rozen

Correspondence

shraddha.shitut@gmail.com (S.S.), d.e.rozen@biology.leidenuniv.nl (D.R.)

In brief

Shitut et al. show how bacterial heterozygosity affects evolution and resistance using an experimental L-form model. Polyploid cells with varied chromosome types survive better across antibiotic gradients. They adjust chromosome ratios to mitigate the costs of antibiotic resistance, revealing new bacterial survival strategies in complex environments.

Highlights

- Bacteria with multiple different chromosomes can survive broad antibiotic exposure
- Heterozygous cells adapt chromosome frequencies in response to external conditions
- Adjusting the chromosome ratio helps heterozygous cells mitigate the cost of resistance
- Heterozygosity boosts adaptive plasticity, like the benefits of multicopy plasmids

Shitut et al., 2025, Current Biology *35*, 1437–1445
April 7, 2025 © 2025 The Author(s). Published by Elsevier Inc.
https://doi.org/10.1016/j.cub.2025.02.012

CellPress

Current Biology

CellPress
OPEN ACCESS

Article

Bacterial heterozygosity promotes survival under multidrug selection

Shraddha Shitut,[1,2,3,4,*] Thomas van Dijk,[2] Dennis Claessen,[2] and Daniel Rozen[2,*]
[1]Origins Centre, Groningen, the Netherlands
[2]Institute of Biology, Leiden University, Sylviusweg 72, 2333 Leiden, the Netherlands
[3]Present address: European Molecular Biology Laboratory, Meyerhofstrasse 1, 69117 Heidelberg, Germany
[4]Lead contact
*Correspondence: shraddha.shitut@gmail.com (S.S.), d.e.rozen@biology.leidenuniv.nl (D.R.)
https://doi.org/10.1016/j.cub.2025.02.012

SUMMARY

Although bacterial cells typically contain a single chromosome, some species are naturally polyploid and carry multiple copies of their chromosome. Polyploid chromosomes can be identical or heterogeneous, the latter giving rise to bacterial heterozygosity. Although the benefits of heterozygosity are well studied in eukaryotes, its consequences in bacteria are less understood. Here, we examine this question in the context of antibiotic resistance to understand how bacterial genomic heterozygosity affects bacterial survival. Using a cell-wall-deficient model system in the actinomycete *Kitasatospora viridifaciens*, we found that heterozygous cells that contain different chromosomes expressing different antibiotic resistance markers persist across a broad range of antibiotic concentrations. Recombinant cells containing the same resistance genes on a single chromosome also survive these conditions, but these cells pay a significant fitness cost due to the constitutive expression of these genes. By contrast, heterozygous cells can mitigate these costs by flexibly adjusting the ratio of their different chromosomes, thereby allowing rapid responses in temporally and spatially variable environments. Our results provide evidence that bacterial heterozygosity can increase adaptive plasticity in bacterial cells in a similar manner to the evolutionary benefits provided by multicopy plasmids in bacteria.

INTRODUCTION

Bacterial cells typically carry a single haploid copy of their genome. Although most bacterial species experience transient polyploidy during exponential cell growth,[1,2] several species, including *Buchnera aphidicola*,[3] *Deinococcus radiodurans*,[4] and *Vibrio cholerae*,[5] contain multiple chromosome copies (polyploidy) as a permanent feature of their life cycle.[6,7] Polyploidy is also observed in several extremophilic archaea,[8] cyanobacteria,[9,10] and so-called giant bacteria[11,12] whose macroscopic cells can contain thousands of chromosomes. In some cases, polyploid chromosomes are identical,[3,13] whereas in other species the chromosomes are heterogeneous.[11,14] This gives rise to a form of bacterial heterozygosity that is analogous to the diversity that originates from allelic heterogeneity in different copies of multicopy plasmids.[15] Experiments and theory have shown that plasmid diversity can accelerate adaptation to stress or competition and improve survival in fluctuating environments.[16–20] At the same time, multicopy plasmids often impose a metabolic burden on host cells that can lead to reduced host fitness (plasmid paradox).[21–23] Despite parallels between multicopy plasmids and chromosomes, the evolutionary consequences of bacterial chromosomal polyploidy and heterozygosity remain poorly understood.[24] Our objective in this study is to address this question using a uniquely tractable experimental system of cell-wall-deficient (CWD or L-form) bacteria derived from the actinomycete *Kitasatospora viridifaciens*.

L-forms are bacterial cells lacking the rigid cell wall that maintains cell shape and structure.[25,26] Cell proliferation occurs through asymmetric processes that result from the interplay of membrane synthesis and biophysical forces.[27–29] Populations of L-forms are highly diverse, with cell volumes that can vary by up to two orders of magnitude (Figure 1A). More importantly, because chromosomal segregation is unregulated, L-form cells vary markedly in chromosomal copy number.[30] This mode of replication and proliferation, together with the fact that L-forms can undergo cell-cell fusion,[31,32] results in extensive polyploidy, where multiple chromosomes coexist within the same cell.

To examine the effects of chromosomal polyploidy and heterozygosity in L-forms, we engineered a pair of chromosomes that could be distinguished by different drug resistance and fluorescent markers.[31] We then generated three combinations (Figure 1B) in which markers were either carried on separate chromosomes in different cells (mixed populations), on a single chromosome (recombinants), or on separate chromosomes within the same cell (heterozygous). Because all our strain types have multiple copies of each chromosome, we use the terms homozygous to indicate cells with only one chromosome type, as present in mixed populations and recombinant cells, and heterozygous to refer to cells with different chromosome types.

This is an open access article under the CC BY license (http://creativecommons.org/licenses/by/4.0/).

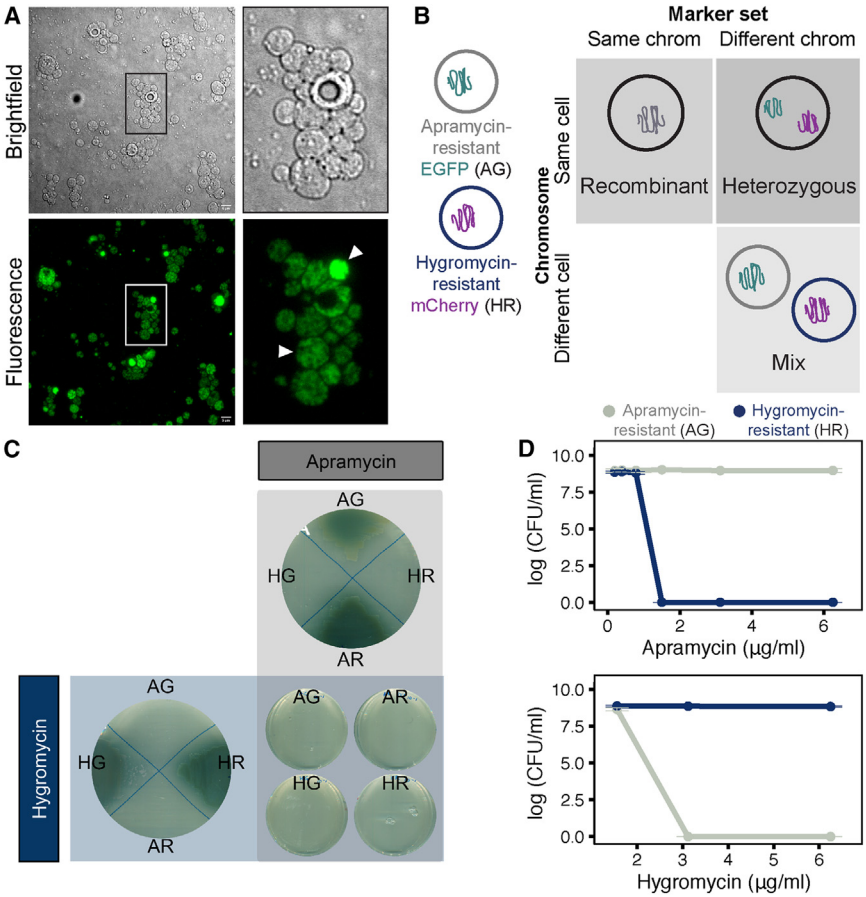

Figure 1. Cell-wall-deficient model system

(A) L-forms of wild-type *K. viridifaciens* have a spherical morphology like other cell-wall-deficient species. Nuclei, when stained with SYTO9 (green), show multiple foci in a single cell (white arrow)—a hallmark of polyploidy.

(B) Schematic of all strain types generated and used in the study. The strains can be grouped based on the chromosome co-occurrence and marker set (apramycin:EGFP and hygromycin:mCherry).

(C) Growth of genetically modified parental L-forms on selective media (apramycin [A], hygromycin [H], EGFP [G], mCherry [R]). AG and AR show growth (green biomass) only on apramycin, whereas HG and HR show growth only on hygromycin. None of the individual strains can grow in media with both antibiotics.

(D) Minimum inhibitory concentration of apramycin (top) and hygromycin (bottom) for parental AG (gray) and HR (navy blue) strains, quantified as colony-forming units/mL (y axis) over a range of tested concentrations (x axis).

See also Figure S1 and Video S1.

We examined the growth and survival of these different populations across a range of antibiotic conditions. Our results provide strong evidence that heterozygous cells persist over a broader range of antibiotic concentrations than homozygous mixed populations. Moreover, we found that heterozygous cells can adaptively adjust chromosomal frequencies—and thus allele ratios—in response to external conditions. This makes it possible for cells to adapt to antibiotic stress while avoiding the metabolic costs of expressing both markers from the same chromosome, as observed in recombinant cells. Our findings indicate that bacterial heterozygosity can benefit cells in fluctuating environments by maintaining genetic diversity, much like multicopy plasmids.

RESULTS

Phenotypic characterization of wall-deficient cells

CWD L-forms of *K. viridifaciens* (Figure 1A) were genetically modified to carry combinations of an antibiotic resistance gene (either conferring resistance to apramycin or hygromycin) and a fluorescence marker gene (either EGFP(G) or mCherry(R)). This resulted in four strains: AG, AR, HG, and HR (Figure 1B). Resistance phenotypes were as expected, with high-level resistance to each respective resistance allele and no cross-resistance (Figure 1C). Apramycin-resistant strains had a minimum inhibitory concentration (MIC) of 3.1 μg/mL for hygromycin, whereas hygromycin-resistant strains had an MIC of 1.6 μg/mL for apramycin (Figure 1D). Neither strain grew on media with both antibiotics (Figure 1C). The AG and HR strains, which show no difference in fitness due to marker introduction (Figure S1), were subsequently fused to create a heterozygous (Het) strain containing both chromosomal types within a single cell (Figure 1B). At the same time, the wild-type strain was consecutively transformed to generate a recombinant (Rec) strain containing all four markers on a single chromosome (Figure 1B).

Growth and fluorescence of the heterozygous (Het), recombinant (Rec), or mixed (Mix) (which refers to a 1:1 mixture of AG and HR monocultures) populations were assessed by spotting 3 μL from a 0.1 OD_{600} culture in different environments varying in the presence or absence of apramycin or hygromycin (Figure 2). In the absence of antibiotics, mixed populations showed patches of either fluorescence color (Figure 2A), with some co-localization of fluorescence across the spot; colocalization was quantified as the correlation between the pixel intensities across the two channels (EGFP and mCherry) (Figure 2, bottom rows). Growth on either antibiotic alone led to monomorphic populations expressing only a single fluorescence marker, indicating that fluorescence is a good proxy for the linked resistance allele. Neither strain in the mixed combination persisted when grown in the presence of inhibitory concentrations of both antibiotics.

By contrast, heterozygous and recombinant cells grew under all antibiotic exposures. In the absence of selection, heterozygous populations showed patches/sectors of both EGFP and mCherry, suggesting either a shift in the ratio of chromosomes containing different markers or chromosomal loss resulting in homozygous lineages. We consider the first possibility in the next section. In the presence of both antibiotics (Figures 2B and 2C, last column), we observed significant colocalization of

CellPress
OPEN ACCESS

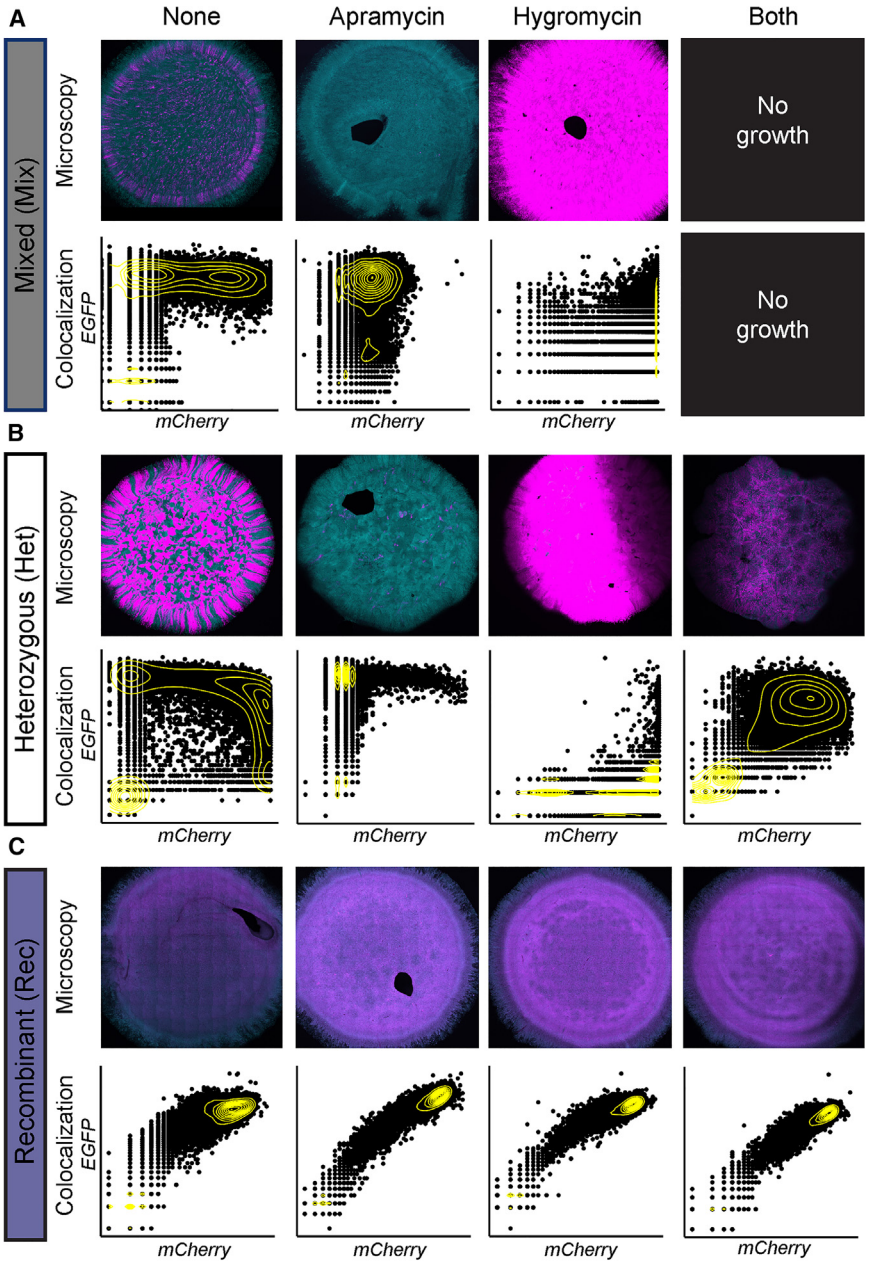

Figure 2. Fluorescence marker expression of strains exposed to different antibiotic treatments

(A–C) Different strain types (A) mixed, (B) heterozygous, and (C) recombinant grown with or without both antibiotics, only apramycin (50 μg/mL), or only hygromycin (100 μg/mL). Fluorescence microscopy of individual colonies (top rows) and the corresponding quantification of fluorescence (bottom rows) show the expression and colocalization of EGFP (cyan) and mCherry (magenta) in different strains in response to selection. Pixel-wise colocalization of either marker in both channels was quantified as signal intensity for each pixel within the colony area. 10,000 randomly sampled points are plotted. A scatter pattern tending toward either the x (mCherry) or y (EGFP) axis indicates dominance of a single marker, whereas a distribution in the top right region indicates colocalization of cells expressing both markers. Yellow contour lines indicate the density of spots. The bottom-left corner, also showing high pixel density, represents pixels in the black background with no fluorescence.

EGFP and mCherry signals across the colony, consistent with the maintenance of both chromosome types (Pearson's $R_{heterozygous}$ = 0.487, $R_{recombinant}$ = 0.885, Figure 2B bottom). During single antibiotic selection, heterozygous populations, like the mixed populations, shifted toward the dominance of a single fluorophore, suggesting that the unselected marker was lost or reduced in frequency (Pearson's $R_{heterozygous}$ = 0.057 [apramycin], $R_{heterozygous}$ = 0.28 [hygromycin]). Recombinant cells grew in all conditions, with significantly more colocalization of the fluorescent markers than heterozygous cells (Pearson's correlation coefficient, ranging from 0.663 to 0.917, Figure 2C bottom). These results again confirm that the strains respond to selection for growth under antibiotic exposure and in terms of fluorescent marker expression.

Heterozygous cells persist across a broad range of antibiotic concentrations

To measure the effects of heterozygosity in more detail, we examined cell growth across a gradient of antibiotic concentrations from 0 to 2× MIC of the parental susceptible population, as shown in the schematic (Figure 3A). The resulting colonies were assessed by quantifying colony-forming units (CFUs) (Figures 3B–3D) and with microscopy (Figures 3E–3G). At sub-MIC concentrations in mixed populations, fluorescence intensity of EGFP and mCherry showed marked deviations, consistent with distinct populations resulting from the loss of the linked drug resistance genes (Figure 3E). We observed only sparse growth at and above the MIC (Figures 3E, dotted box, and S2A).

By contrast, heterozygous cells grew well in all antibiotic concentrations (Figures 3B–3D). The benefit of chromosomal diversity in heterozygous cells is shown in two ways. First, we observed a significant relative advantage of heterozygous versus mixed cells in terms of CFU (Figures 3B–3D, Welch t test). Second, in contrast to mixed populations, heterozygous cells grew well in the presence of both antibiotics at concentrations at and above the MIC, as indicated by correlated patches of both fluorescent markers (Figures 3F and S2B). Interestingly, the advantage to heterozygous cells was observed both above and below the MIC for single and double antibiotic exposure. This indicates that heterozygous cells grow better over a broader environmental range than either genotype in the mixed populations and suggests that heterozygous cells do not pay a

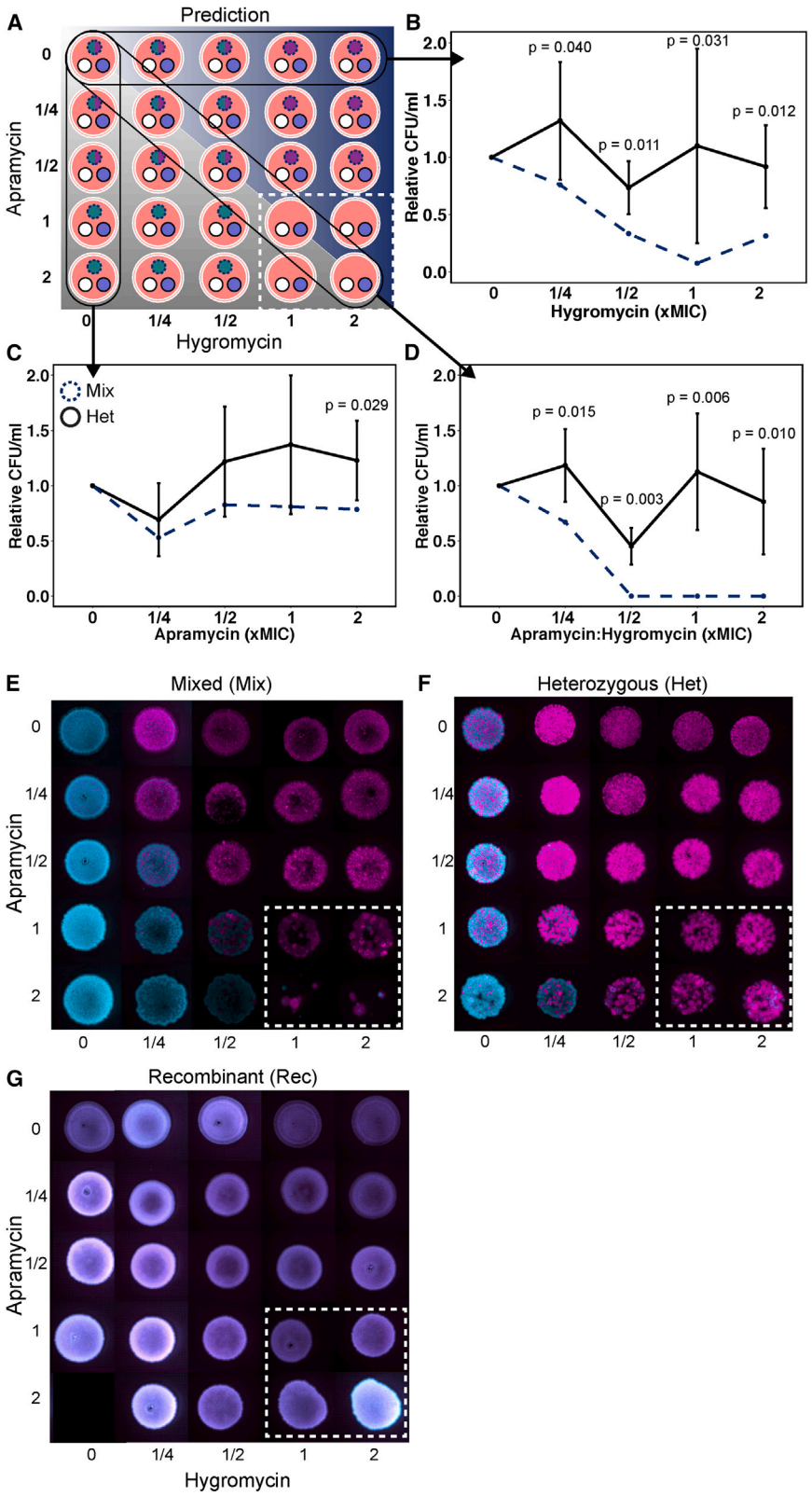

Figure 3. Growth advantage of heterozygous cells in different antibiotic concentrations

(A) Experimental setup of individual plates consisting of varying concentrations of apramycin and hygromycin below and above the MIC (0–2×). Each plate was inoculated with three strains (mixed [dotted circle], heterozygous [smooth white circle], and recombinant [smooth purple circle]). Each spot represents the predicted growth (presence or absence) and fluorescence expression (cyan for EGFP and magenta for mCherry).

(B–D) After 3 days of growth, appropriate dilutions were used to quantify cell numbers by plating. Heterozygous populations (bold lines) show growth at all concentrations, whereas mixed populations do not (dotted lines). Significant differences are reported for each tested pair of heterozygous and mixed populations (Welch t test, $n = 3$).

(E–G) Fluorescence images of colonies after 3 days of incubation. (E) The mixed (Mix) strain grows well below MIC, with either EGFP or mCherry expression corresponding to the antibiotic selection. Growth is significantly reduced or absent when exposed to both antibiotics above the MIC (dotted white box). (F) The heterozygous (Het) strain can grow equally well across the gradient below and above MIC. Markers not under selection are visible in patches, consistent with shifts in chromosome/allele frequencies. (G) The recombinant (Rec) strain grew similarly across the antibiotic gradient, with equal expression of EGFP and mCherry.

See also Figures S2 and S3.

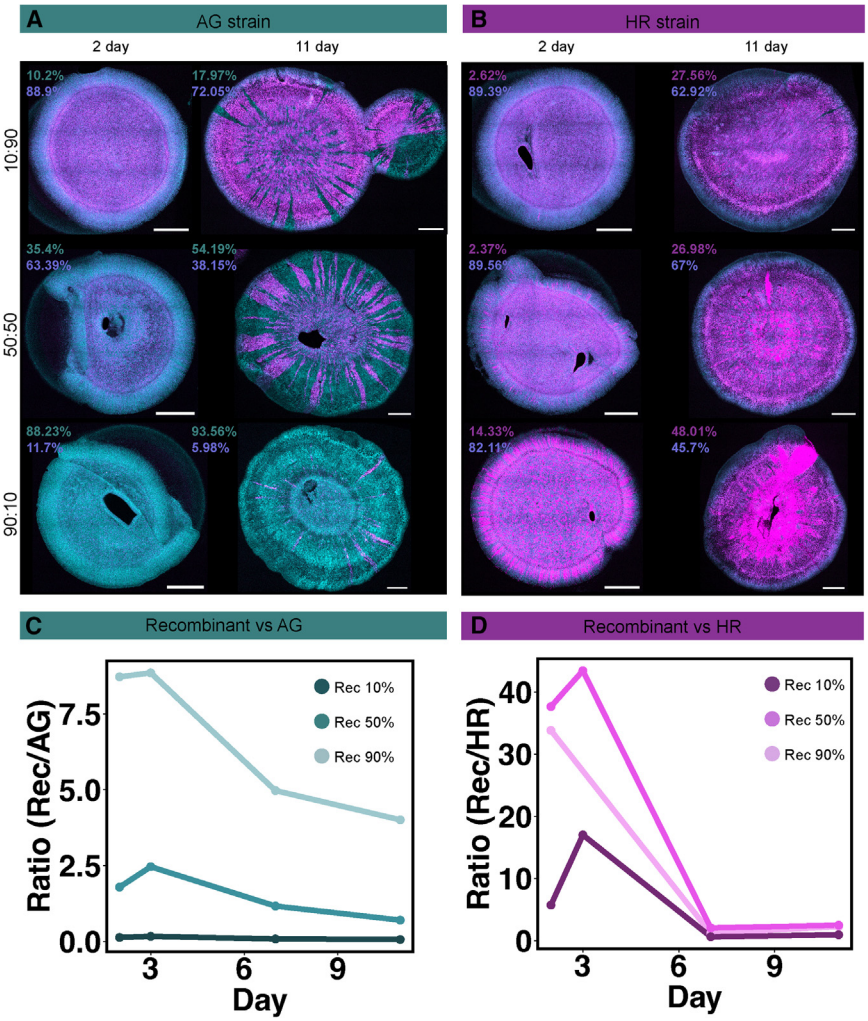

Figure 4. Fitness cost for recombinant cells

Parental strains (A) AG or (B) HR were mixed with the recombinant (Rec) in different starting ratios (10:90, 50:50, and 90:10) and incubated for 11 days. Fluorescence microscopy of individual colonies at different time points (representative images from days 2 and 11 are shown) was used to quantify the ratio of EGFP (cyan) and mCherry (magenta) expressing cells, indicated as percentages next to the colony image. Scale bars indicate 100 micrometer. Based on this measurement, the ratio of (C) Rec to AG or (D) Rec to HR was calculated over time, with the recombinant declining at all inoculation frequencies.
See also Figure S3.

fitness cost for maintaining both chromosome types, even below the MIC.

Recombinant colonies grew at all antibiotic concentrations with a uniform expression of both fluorescence markers (Figures 3G and S2C) and similar biomass (in terms of area) compared with the heterozygous and mixed populations (Figure S2D). However, comparing the morphology of recombinant colonies with heterozygous colonies, the growth of heterozygous cells in colonies is less spatially uniform, suggesting the possible loss or skew in frequencies of either chromosome type leading to cell death (Figure S3).

Fixed versus flexible costs of antibiotic resistance

An important difference between heterozygous and recombinant cells is that the latter constitutively expresses both markers from a single chromosome. To quantify possible costs of this expression in recombinant cells, we estimated the fitness of the recombinant strain when competing against either parental strain: AG (Figure 4A) or HR (Figure 4B). Consistent with a significant metabolic cost to antibiotic resistance, we observed that the recombinant strain was rapidly outcompeted by the parent strains (Figure 4C), regardless of the initial frequencies (10:90, 50:50, or 90:10).

In contrast to the fixed fitness costs observed in recombinant strains, we tested whether these costs could be mitigated in heterozygous cells by flexibly altering chromosome (resistance allele) ratios in response to external conditions.[18,19] To examine this possibility, we used quantitative PCR to quantify the frequencies of antibiotic resistance markers (*aac(3)IV* and *hph* for the apramycin and hygromycin resistance genes, respectively, Figure S5) in mixed, heterozygous, and recombinant cells grown across a gradient of both antibiotics.

Our results show how the frequency of each antibiotic resistance gene changes in the three cell types after exposure to different antibiotic concentrations (Figure 5). These results lead to the following conclusions. First, antibiotic resistance gene frequencies are responsive to environmental conditions (Figures 5A–5C). At the highest concentrations of either antibiotic (Figure 5D blue and gray box), mixed and heterozygous populations showed strongly skewed frequencies of each resistance allele. In the mixed population, this skew was due to selection of either resistant strain by the corresponding antibiotic and the extinction of the other. By contrast, in the heterozygous cells, selection acted between chromosomes within each cell, resulting in a skewed chromosomal ratio at the per-cell level that corresponded predictably to the associated antibiotic exposure (Figure 5B). Importantly, this shift in antibiotic selection caused an almost complete loss of viability in the mixed population above MIC (Figure 3), whereas heterozygous cells retained normal growth. Second, although resistance markers in mixed populations were entirely lost during exposure to the higher concentrations of either antibiotic (ranging from 0% to 100%), they were maintained in heterozygous cells across all drug exposure conditions (ranging from ~3% to 97%) (Figure 5D). Thus, although growth of mixed populations was curtailed due to the loss of functional diversity, the maintenance of both alleles in heterozygous cells permitted their growth across a broader environmental range compared with the mixed population. Resistance gene frequencies in recombinant cells were

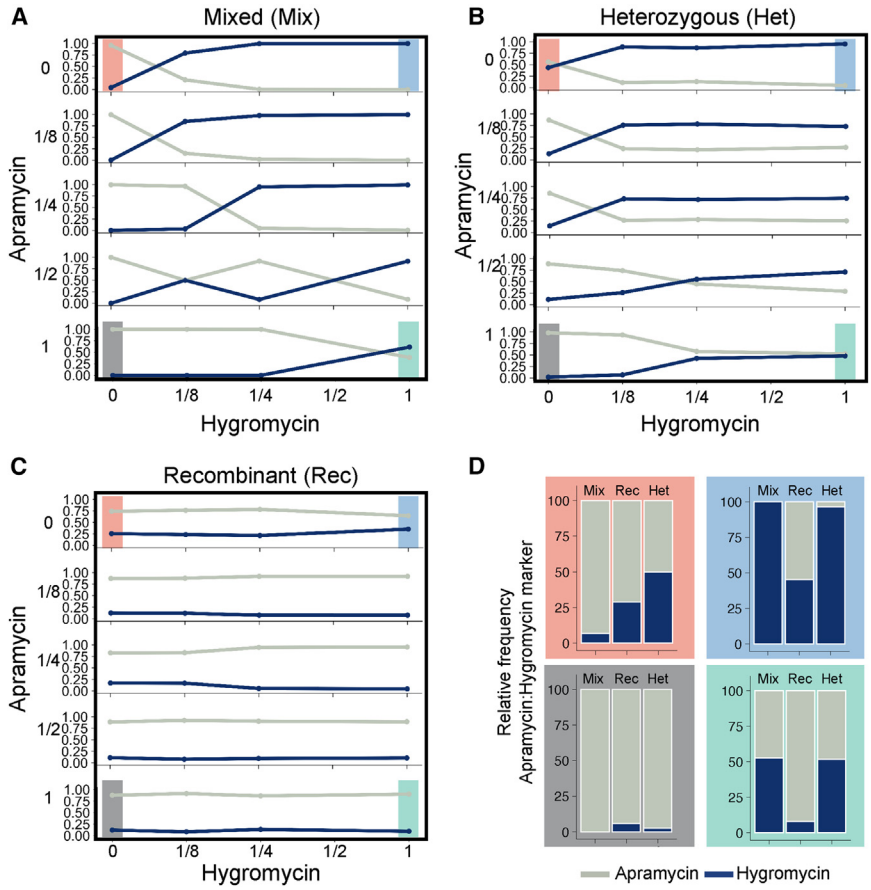

Figure 5. Marker ratio change over the selection gradient

(A–C) The frequency of apramycin and hygromycin resistance markers was quantified via qPCR from the collected biomass of mixed (Mix), recombinant (Rec), and heterozygous (Het) populations. The frequency of the apramycin (gray) to hygromycin (blue) marker shows different patterns across the gradient of selection for the mixed and heterozygous populations, whereas the frequency in recombinant populations is similar across antibiotic exposure levels.

(D) Marker proportions at the extreme antibiotic concentrations show the maintenance of both antibiotic resistance genes in the heterozygous population, even at extreme concentrations of either antibiotic alone. In the highest hygromycin region (blue box), the apramycin marker (gray bar) is maintained, and in the apramycin high region (gray box), the hygromycin marker (navy blue bar) is maintained. This shows that the heterozygous population retains both resistance markers, even under extreme selective pressure.

See also Figure S5.

comparatively similar, regardless of antibiotic exposure and associated costs (Figure 5C).

Chromosome frequencies in heterozygous cells segregate in temporal and spatial antibiotic gradients

Resources and stress vary spatially and temporally in natural environments. To test whether heterozygous cells could flexibly adjust chromosome ratios to persist in these dynamic environments, we examined growth and fluorescence (indicative of allele frequencies) on plates with opposing antibiotic gradients (Figure 6A). We used paper disks to create opposing antibiotic selection gradients in the same environment. Because diffusion from paper disks containing antibiotics occurs continuously over time, this approach allowed us to analyze the effects of heterozygosity as the colony grew.

Three days after cells were inoculated onto plates with opposing antibiotic gradients, heterozygous cells experienced a high concentration of one antibiotic and a low concentration of the other. As expected, fluorescence intensities initially corresponded to the level of drug exposure (Figure 6B): cells grown near apramycin (shown in cyan) predominantly expressed EGFP (75%), whereas cells grown near hygromycin (shown in magenta) overwhelmingly expressed mCherry (97%) (Figure 6C). However, after 15 days, during which time the concentration of both antibiotics changed due to diffusion, we observed a corresponding shift in fluorescence expression owing to the persistence of both resistance genes. As the concentration of hygromycin declined, so did the expression of mCherry (from 97% to 80%). At the same time, because cells were increasingly exposed to apramycin, there was a corresponding increase in the expression of EGFP (from 0.6% to ~9%). The same qualitative response was seen in cells initially grown closer to apramycin. As the concentration of apramycin decreased, the expression of EGFP also decreased (by 22.4%), whereas as hygromycin selection increased, the expression of mCherry increased (by 21.8%). For both cases (biomass initially close to hygromycin or close to apramycin), the fraction of double-labeled cells increased most visibly on the side of the colony exposed to both antibiotics (white arrows).

Parallel experiments in antibiotic gradients were carried out with mixed and recombinant populations (Figure S4A). As expected, mixed populations show enrichment of either cell type, depending on the antibiotic; however, both colonies were growth arrested over 15 days due to the diffusion of drugs (Figure S4B). Recombinant cells grew over the 15-day period, but their marker expression and change in marker expression were the same irrespective of proximity to either antibiotic disc (Figure S4C).

DISCUSSION

Bacterial polyploidy creates opportunities to increase phenotypic and genetic diversity within a single cell by retaining multiple chromosomal copies.[14,15,33,34] To understand the evolutionary consequences of this increased diversity, we used cell-cell fusion in *K. viridifaciens* L-forms to create heterozygous lineages that were then examined across fixed and dynamic gradients of antibiotics. Our results show that heterozygosity allows cells to persist across a broader range of antibiotic concentrations than a mixed population of homozygous cells, likely owing

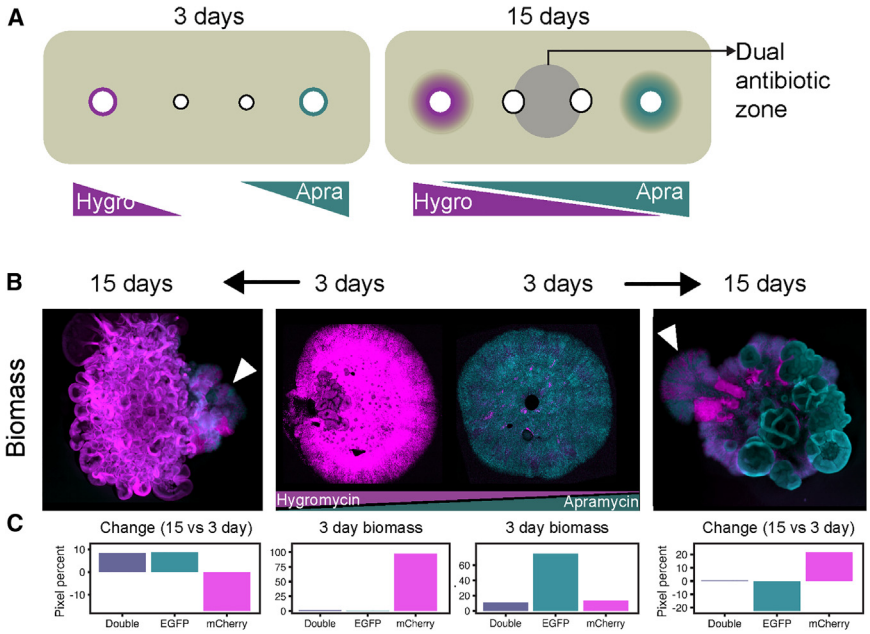

Figure 6. Marker frequencies in heterozygous populations growing in antibiotic selection gradients are dynamic

(A) The antibiotic gradient was set up in the same environment by placing filter discs (filled white circles with colored outline) containing antibiotics such that they diffused into the agar medium, indicated by the gray halo. Populations were inoculated in the center (filled white circles with black outline), thus experiencing an increasing gradient of a different antibiotic on each side.

(B) The response of a heterozygous population when exposed to an opposing gradient of hygromycin and apramycin. Colonies were measured after 3 and 15 days and quantified for each fluorescent marker. mCherry (magenta) was used as a marker for the hygromycin gradient, and EGFP (cyan) was used as a marker for the apramycin gradient. White arrows indicate regions of double-labeled cells.

(C) At 3 days, the fluorescence pixel percent correlated with the antibiotic selection, with high mCherry (97%) near the hygromycin gradient and high EGFP (75%) near the apramycin gradient. From 3 to 15 days, the fluorescence pixel percent showed an opposite trend, with an increase in EGFP (8.8%) near the hygromycin gradient and an increase in mCherry (21.8%) near the apramycin gradient.

See also Figure S4.

to the persistence of both resistance genes in these cells. In addition, we found that heterozygous cells can mitigate the costs of antibiotic resistance by flexibly adjusting the frequency of resistance genes to match external drug exposure. This response occurs rapidly in the presence of a static antibiotic concentration and dynamically in response to a shifting antibiotic gradient. Together, our results suggest that the plasticity provided by chromosome heterozygosity may facilitate bacterial adaptation to environmental heterogeneity or stress.

The benefits of bacterial heterozygosity mirror the effects of analogous systems in bacteria that increase genetic diversity,[2,11] gene expression,[35] or protein abundance[36] through increased copy number. For individual genes or smaller chromosomal regions, tandem gene amplifications can lead to antibiotic heteroresistance.[2,16,37] This allows otherwise susceptible cells to become transiently drug tolerant while also increasing the number of mutational targets that can lead to more stable resistance. Multicopy plasmids offer similar benefits in high antibiotic concentrations or across fluctuating environments with varying levels of antibiotic exposure.[15]

In each of these analogous systems, the benefits afforded by increased copy number or gene expression allow flexible and plastic responses whose effects are more rapid than genetic changes via mutation.[16,18] At the same time, the costs of overexpression or plasmid carriage ensure that these processes are transient and highly variable across bacterial populations. Heteroresistance is only observed in a minor fraction of bacterial cells, whereas plasmid copy number can vary markedly depending on the concentration or frequency of antibiotic exposure.[16,37] Similarly, our results suggest that the benefits of chromosome heterozygosity are not consistent across all conditions and may also be transient. During antibiotic exposure, chromosome copy number can rapidly shift to increase the frequency of the appropriate resistance gene. However, just as tandem duplications and plasmids are lost, so too are chromosomes due to unequal segregation during cell division.[38] As far as we are aware, there are no mechanisms to ensure reliable chromosome partitioning or copy number in L-form cells, although these may be present in naturally polyploid species. In L-forms, segregational loss can potentially be overcome by cell-cell fusion that would recreate a new heterozygous lineage (Video S1).[31,32,39,40] This type of fusion and segregation is thought to have been a major driver of the adaptability of protocells that existed before the evolution of the more rigid bacterial cell wall.[26]

Numerous processes have evolved to provide microbial populations with the ability to generate adaptive plasticity in response to environmental stress or instability. Our results suggest that chromosomal heterozygosity offers bacteria yet another mechanism to flexibly respond to shifting environments. Further work in related systems and in naturally polyploid bacterial species will be needed to assess how widespread this phenomenon is across microbial groups and environments.

RESOURCE AVAILABILITY

Lead contact

Requests for further information and resources should be directed to and will be fulfilled by the lead contact, Shraddha Shitut (shraddha.shitut@gmail.com).

Materials availability

This study did not generate new unique reagents. Strains generated for this study will be made available upon request, with reasonable compensation for their processing and shipping.

Data and code availability

- Data: all other data reported in this paper will be shared by the lead contact upon request.
- Code: this paper does not report original code.

- Additional information: any additional information required to reanalyze the data reported in this paper is available from the lead contact upon request.

ACKNOWLEDGMENTS

We thank members of the Rozen and Claessen labs for fruitful discussions and suggestions. S.S. acknowledges Samir Giri and Jordi van Gestel for comments on the manuscript. S.S. was supported by the Origins Centre (NWA impulse) for funding. T.v.D. acknowledges NWO for funding. D.C. and D.R. were supported by the Dutch Science Foundation (NWO: ALW).

AUTHOR CONTRIBUTIONS

Conceptualization, S.S., D.C., and D.R.; methodology, S.S. and T.v.D.; investigation, S.S., T.v.D., and D.R.; writing – original draft, S.S.; writing – review and editing, S.S., D.C., and D.R.; funding acquisition, S.S., D.C., and D.R.; supervision, D.C. and D.R.

DECLARATION OF INTERESTS

The authors declare no competing interests.

STAR★METHODS

Detailed methods are provided in the online version of this paper and include the following:

- KEY RESOURCES TABLE
- EXPERIMENTAL MODEL AND STUDY PARTICIPANT DETAILS
  - Strains and media
- METHOD DETAILS
  - Minimum inhibitory concentration (MIC) quantification
  - Competition experiment
  - Cell growth across a range of antibiotic concentrations
  - Microscopy and image analysis
  - Quantitative PCR-based chromosome ratio estimation
  - Resistance and growth in antibiotic gradients
- QUANTIFICATION AND STATISTICAL ANALYSIS

SUPPLEMENTAL INFORMATION

Supplemental information can be found online at https://doi.org/10.1016/j.cub.2025.02.012.

Received: May 23, 2024
Revised: November 21, 2024
Accepted: February 5, 2025
Published: March 3, 2025

REFERENCES

1. Maldonado, R., Jiménez, J., and Casadesús, J. (1994). Changes of ploidy during the Azotobacter vinelandii growth cycle. J. Bacteriol. *176*, 3911–3919. https://doi.org/10.1128/jb.176.13.3911-3919.1994.
2. Sun, L., Alexander, H.K., Bogos, B., Kiviet, D.J., Ackermann, M., and Bonhoeffer, S. (2018). Effective polyploidy causes phenotypic delay and influences bacterial evolvability. PLoS Biol. *16*, e2004644. https://doi.org/10.1371/journal.pbio.2004644.
3. Shigenobu, S., Watanabe, H., Hattori, M., Sakaki, Y., and Ishikawa, H. (2000). Genome sequence of the endocellular bacterial symbiont of aphids Buchnera sp. APS. Nature *407*, 81–86. https://doi.org/10.1038/35024074.
4. Zahradka, K., Slade, D., Bailone, A., Sommer, S., Averbeck, D., Petranovic, M., Lindner, A.B., and Radman, M. (2006). Reassembly of shattered chromosomes in Deinococcus radiodurans. Nature *443*, 569–573. https://doi.org/10.1038/nature05160.
5. Paranjape, S.S., and Shashidhar, R. (2017). The ploidy of Vibrio cholerae is variable and is influenced by growth phase and nutrient levels. FEMS Microbiol. Lett. *364*, fnx190. https://doi.org/10.1093/femsle/fnx190.
6. Soppa, J. (2014). Polyploidy in Archaea and Bacteria: About Desiccation Resistance, Giant Cell Size, Long-Term Survival, Enforcement by a Eukaryotic Host and Additional Aspects. Microbial Physiology. J. Mol. Microbiol. Biotechnol. *24*, 409–419. https://doi.org/10.1159/000368855.
7. Pecoraro, V., Zerulla, K., Lange, C., and Soppa, J. (2011). Quantification of Ploidy in Proteobacteria Revealed the Existence of Monoploid, (Mero-) Oligoploid and Polyploid Species. PLoS ONE *6*, e16392. https://doi.org/10.1371/journal.pone.0016392.
8. Soppa, J. (2013). Evolutionary advantages of polyploidy in halophilic archaea. Biochem. Soc. Trans. *41*, 339–343. https://doi.org/10.1042/BST20120315.
9. Griese, M., Lange, C., and Soppa, J. (2011). Ploidy in cyanobacteria. FEMS Microbiol. Lett. *323*, 124–131. https://doi.org/10.1111/j.1574-6968.2011.02368.x.
10. Weissenbach, J., Aguilera, A., Bas Conn, L., Pinhassi, J., Legrand, C., and Farnelid, H. (2024). Ploidy levels in diverse picocyanobacteria from the Baltic Sea. Environ. Microbiol. Rep. *16*, e70005. https://doi.org/10.1111/1758-2229.70005.
11. Ionescu, D., Zoccarato, L., Zaduryan, A., Schorn, S., Bizic, M., Pinnow, S., Cypionka, H., and Grossart, H.-P. (2021). Heterozygous, Polyploid, Giant Bacterium, Achromatium, Possesses an Identical Functional Inventory Worldwide across Drastically Different Ecosystems. Mol. Biol. Evol. *38*, 1040–1059. https://doi.org/10.1093/molbev/msaa273.
12. Ionescu, D., Volland, J.-M., Contarini, P.-E., and Gros, O. (2023). Genomic Mysteries of Giant Bacteria: Insights and Implications. Genome Biol. Evol. *15*, evad163. https://doi.org/10.1093/gbe/evad163.
13. Atsushi, N., and Moran Nancy, A. (2022). Extreme Polyploidy of Carsonella, an Organelle-Like Bacterium with a Drastically Reduced Genome. Microbiol. Spec. *10*, e0035022. https://doi.org/10.1128/spectrum.00350-22.
14. Maurya, G.K., Chaudhary, R., Pandey, N., and Misra, H.S. (2021). Molecular insights into replication initiation in a multipartite genome harboring bacterium Deinococcus radiodurans. J. Biol. Chem. *296*, 100451. https://doi.org/10.1016/j.jbc.2021.100451.
15. San Millan, A., Escudero, J.A., Gifford, D.R., Mazel, D., and MacLean, R.C. (2016). Multicopy plasmids potentiate the evolution of antibiotic resistance in bacteria. Nat. Ecol. Evol. *1*, 10. https://doi.org/10.1038/s41559-016-0010.
16. Hernandez-Beltran, J.C.R., Rodríguez-Beltrán, J., Aguilar-Luviano, O.B., Velez-Santiago, J., Mondragón-Palomino, O., MacLean, R.C., Fuentes-Hernández, A., San Millán, A., and Peña-Miller, R. (2024). Plasmid-mediated phenotypic noise leads to transient antibiotic resistance in bacteria. Nat. Commun. *15*, 2610. https://doi.org/10.1038/s41467-024-45045-0.
17. Heuer, H., and Smalla, K. (2012). Plasmids foster diversification and adaptation of bacterial populations in soil. FEMS Microbiol. Rev. *36*, 1083–1104. https://doi.org/10.1111/j.1574-6976.2012.00337.x.
18. Santer, M., Kupczok, A., Dagan, T., and Uecker, H. (2022). Fixation dynamics of beneficial alleles in prokaryotic polyploid chromosomes and plasmids. Genetics *222*, iyac121. https://doi.org/10.1093/genetics/iyac121.
19. Rodriguez-Beltran, J., Hernandez-Beltran, J.C.R., DelaFuente, J., Escudero, J.A., Fuentes-Hernandez, A., MacLean, R.C., Peña-Miller, R., and San Millan, A. (2018). Multicopy plasmids allow bacteria to escape from fitness trade-offs during evolutionary innovation. Nat. Ecol. Evol. *2*, 873–881. https://doi.org/10.1038/s41559-018-0529-z.
20. Rodríguez-Beltrán, J., Sørum, V., Toll-Riera, M., de la Vega, C., Peña-Miller, R., and San Millán, Á. (2020). Genetic dominance governs the evolution and spread of mobile genetic elements in bacteria. Proc. Natl. Acad. Sci. USA *117*, 15755–15762. https://doi.org/10.1073/pnas.2001240117.

21. Alvaro, S.M., and Craig, M.R. (2017). Fitness Costs of Plasmids: a Limit to Plasmid Transmission. Microbiol. Spec. *5*. https://doi.org/10.1128/microbiolspec.mtbp-0016–2017.

22. Harrison, E., and Brockhurst, M.A. (2012). Plasmid-mediated horizontal gene transfer is a coevolutionary process. Trends Microbiol. *20*, 262–267. https://doi.org/10.1016/j.tim.2012.04.003.

23. Brockhurst, M.A., and Harrison, E. (2022). Ecological and evolutionary solutions to the plasmid paradox. Trends Microbiol. *30*, 534–543. https://doi.org/10.1016/j.tim.2021.11.001.

24. Markov, A.V., and Kaznacheev, I.S. (2016). Evolutionary consequences of polyploidy in prokaryotes and the origin of mitosis and meiosis. Biol. Direct *11*, 28. https://doi.org/10.1186/s13062-016-0131-8.

25. Allan, E.J., Hoischen, C., and Gumpert, J. (2009). Chapter 1 Bacterial L-Forms. In Advances in Applied Microbiology, *68* (Academic Press), pp. 1–39. https://doi.org/10.1016/S0065-2164(09)01201-5.

26. Errington, J., Mickiewicz, K., Kawai, Y., and Wu, L.J. (2016). L-form bacteria, chronic diseases and the origins of life. Philos. Trans. R. Soc. Lond. B Biol. Sci. *371*, 20150494. https://doi.org/10.1098/rstb.2015.0494.

27. Leaver, M., Domínguez-Cuevas, P., Coxhead, J.M., Daniel, R.A., and Errington, J. (2009). Life without a wall or division machine in Bacillus subtilis. Nature *457*, 849–853. https://doi.org/10.1038/nature07742.

28. Mercier, R., Kawai, Y., and Errington, J. (2014). General principles for the formation and proliferation of a wall-free (L-form) state in bacteria. eLife *3*, e04629. https://doi.org/10.7554/eLife.04629.

29. Studer, P., Staubli, T., Wieser, N., Wolf, P., Schuppler, M., and Loessner, M.J. (2016). Proliferation of Listeria monocytogenes L-form cells by formation of internal and external vesicles. Nat. Commun. *7*, 13631. https://doi.org/10.1038/ncomms13631.

30. Ramijan, K., Ultee, E., Willemse, J., Zhang, Z., Wondergem, J.A.J., van der Meij, A., Heinrich, D., Briegel, A., van Wezel, G.P., and Claessen, D. (2018). Stress-induced formation of cell wall-deficient cells in filamentous actinomycetes. Nat. Commun. *9*, 5164. https://doi.org/10.1038/s41467-018-07560-9.

31. Shraddha, S., Meng-Jie, S., Bart, C., Derks Rico, J.E., Martin, G., Daniel, R., Dennis, C., and Alexander, K. (2022). Generating Heterokaryotic Cells via Bacterial Cell-Cell Fusion. Microbiol. Spec. *10*, e0169322. https://doi.org/10.1128/spectrum.01693-22.

32. Naor, A., and Gophna, U. (2013). Cell fusion and hybrids in Archaea. null. Bioengineered *4*, 126–129. https://doi.org/10.4161/bioe.22649.

33. Hansen, M.T. (1978). Multiplicity of genome equivalents in the radiation-resistant bacterium Micrococcus radiodurans. J. Bacteriol. *134*, 71–75. https://doi.org/10.1128/jb.134.1.71-75.1978.

34. Tobiason, D.M., and Seifert, H.S. (2006). The Obligate Human Pathogen, Neisseria gonorrhoeae, Is Polyploid. PLoS Biol. *4*, e185. https://doi.org/10.1371/journal.pbio.0040185.

35. Komaki, K., and Ishikawa, H. (2000). Genomic copy number of intracellular bacterial symbionts of aphids varies in response to developmental stage and morph of their host. Insect Biochem. Mol. Biol. *30*, 253–258. https://doi.org/10.1016/S0965-1748(99)00125-3.

36. Hinzke, T., Kleiner, M., Meister, M., Schlüter, R., Hentschker, C., Pané-Farré, J., Hildebrandt, P., Felbeck, H., Sievert, S.M., Bonn, F., et al. (2021). Bacterial symbiont subpopulations have different roles in a deep-sea symbiosis. eLife *10*, e58371. https://doi.org/10.7554/eLife.58371.

37. Nicoloff, H., Hjort, K., Levin, B.R., and Andersson, D.I. (2019). The high prevalence of antibiotic heteroresistance in pathogenic bacteria is mainly caused by gene amplification. Nat. Microbiol. *4*, 504–514. https://doi.org/10.1038/s41564-018-0342-0.

38. Garoña, A., Santer, M., Hülter, N.F., Uecker, H., and Dagan, T. (2023). Segregational drift hinders the evolution of antibiotic resistance on polyploid replicons. PLoS Genet. *19*, e1010829. https://doi.org/10.1371/journal.pgen.1010829.

39. Ogle, B.M., Cascalho, M., and Platt, J.L. (2005). Biological implications of cell fusion. Nat. Rev. Mol. Cell Biol. *6*, 567–575. https://doi.org/10.1038/nrm1678.

40. Küppers, G., and Zimmermann, U. (1983). Cell fusion by spark discharge and its relevance for evolutionary processes. FEBS Lett. *164*, 323–329. https://doi.org/10.1016/0014-5793(83)80310-X.

41. Schindelin, J., Arganda-Carreras, I., Frise, E., Kaynig, V., Longair, M., Pietzsch, T., Preibisch, S., Rueden, C., Saalfeld, S., Schmid, B., et al. (2012). Fiji: an open-source platform for biological-image analysis. Nat. Methods *9*, 676–682. https://doi.org/10.1038/nmeth.2019.

42. R Core Team (2014). R: A Language and Environment for Statistical Computing (R Foundation for Statistical Computing).

43. Combes, P., Till, R., Bee, S., and Smith, M.C.M. (2002). The Streptomyces Genome Contains Multiple Pseudo-attB Sites for the ϕC31-Encoded Site-Specific Recombination System. J. Bacteriol. *184*, 5746–5752. https://doi.org/10.1128/JB.184.20.5746-5752.2002.

STAR★METHODS

KEY RESOURCES TABLE

REAGENT or RESOURCE	SOURCE	IDENTIFIER
Bacterial and virus strains		
Kitasatospora viridifaciens AG	Shitut et al.[31]	N/A
Kitasatospora viridifaciens HR	Shitut *et al*[31]	N/A
Chemicals, peptides, and recombinant proteins		
Apramycin sulphate	Duchefa Biochemie	Catalog #A0164
Hygromycine B	Duchefa Biochemie	Catalog #H0192
Polyethylene glycol 1000	NBS Biologicals	N/A (discontinued)
Critical commercial assays		
iTaq Universal SYBRGreen Supermix kit	Biorad	Catalog #1725121
Experimental models: Organisms/strains		
Kitasatospora viridifaciens	Ramijan et al.[30]	N/A
Oligonucleotides		
Primer- infB_fwd 5' CGAAACGCCAGGAATATGAAG 3'	This paper	N/A
Primer- infB_rev 5' CGCCCAGGTTAAACATCAC 3'	This paper	N/A
Primer- apr_fwd 5' GCAATACGAATGGCGAAAAG 3'	This paper	N/A
Primer- apr_rev 5' AGATGATCTGCTCTGCCTG 3'	This paper	N/A
Primer- hyg_fwd 5' ACCGTGCTCACCCCCCATTC 3'	This paper	N/A
Primer- hyg_rev 5' CCGGAAGGCGTTGAGATGCAG 3'	This paper	N/A
Software and algorithms		
ImageJ/Fiji	Schindelin et al.[41]	https://doi.org/10.1038/nmeth.2019
R Studio	R Core Team[42]	https://github.com/rstudio/rstudio

EXPERIMENTAL MODEL AND STUDY PARTICIPANT DETAILS

Strains and media

Apramycin resistant:GFP (AG) and hygromycin resistant:mCherry (HR) lines of *K. viridifaciens* DSM40239 were used from a previous study which details the strain construction.[31] Briefly, plasmids containing the marker combinations along with a phiC31 *attP* site and integrase gene were introduced into L-forms via PEG-induced transformation. The resultant transformants were directly selected on antibiotic containing media. For the fusion strain, a poly(ethylene) glycol (10%) mediated fusion was used to fuse AG with HR followed by two rounds of selection on both antibiotics. The resultant strain contains different chromosome types in the same cell with the marker sets on separate chromosomes. The recombinant strain was obtained by transforming a wild-type *K. viridifaciens* L-form with both sets of markers in consecutive steps such that insertion takes place on the same chromosome (Figure 1B). Transformation was carried out using a modified protoplast transformation protocol using plasmids containing the two marker sets. The first insertion takes place at the *attP* site (via phiC31 integrase) and the second insertion potentially occurs at a *pseudo-attP* site.[43] This recombinant strain contains all marker sets on the same chromosome and was enriched by selection on plates containing both antibiotics at least 3 times. All strains were grown on L-phase broth (LPB) which consists of a 1:1 mixture of yeast extract malt extract and tryptic soy broth supplemented with 10% sucrose and 25 mM $MgCl_2$. Colony growth for quantification and imaging was done on L-phase agar (LPMA) which is LPB containing 1.5% agar, 5% horse serum and 25 mM $MgCl_2$. Apramycin and hygromycin (Duchefa Biochemie) were added as per experimental requirement and all incubations were carried out at 30°C.

METHOD DETAILS

Minimum inhibitory concentration (MIC) quantification

Monocultures of AG and HR were grown in LPB for 3 days from a stock culture. These cultures were adjusted to 0.1 OD_{600} and spot diluted (1:10 over 6 rounds) on LPMA plates containing increasing amounts of antibiotics. For apramycin the range tested was (in decreasing order): 6.25, 3.12, 1.56, 0.78, 0.39, 0.19 μg/ml. For hygromycin the range tested was (in decreasing order): 50, 25, 12.5, 6.25, 3.12 and 1.56 μg/ml. Both strains were plated on all concentrations and incubated for 3 days. Colonies in spots were counted and CFU/ml was quantified.

Competition experiment

Pairwise mixes of OD_{600} adjusted cultures were prepared with varying ratios of parent (AG or HR) to recombinant strains (10:90, 50:50 and 90:10), to control for frequency-dependent effects. Each mix was spotted onto media without antibiotic selection to test for the cost of carrying resistance markers. The spot was allowed to grow over 11 days and imaging was done at day 2 (colonies become visible), 3, 7 and 11. Images were processed and analysed for percentage of pixels in both channels (EGFP and mCherry) to track the parental population over time. The single channel pixel percent (EGFP or mCherry) tracks the parental strain ratio while the overlapping pixel percent (EGFP and mCherry) is representative of the recombinant strain.

Cell growth across a range of antibiotic concentrations

Population growth (fused and mixed) was tested across a range of antibiotic concentrations (0, ¼, ½, 1 and 2x MIC of apramycin and hygromycin). Cell culture of 3 μl in the form of a spot was grown at each specified antibiotic concentration in a plate consisting of defined concentrations of apramycin and hygromycin as shown in Figure 3A. Each condition and strain were tested in triplicate. After 3 days of growth at 30°C we quantified CFU/ml using the appropriate dilution and isolated single colonies for microscopic analysis.

Microscopy and image analysis

Whole colony imaging was done by cutting out and flipping the colony into an Ibidi→ 8-well chamber slide. A Zeiss LSM 900 Airyscan 2 microscope with an inverted objective was employed to visualize the fluorescently labelled microbial strains at a magnification of 40x. EGFP strains (AG, Rec, Fused) were excited at a wavelength of 488 nm, with emission detection at 535 nm. Conversely, the mCherry strains (HR, Rec, Fused) were excited at 535 nm, and its emission was captured at 650 nm. Utilizing the Zen software developed by Zeiss, we acquired multichannel images encompassing both fluorescence and bright-field signals in a multistack format. These images were subsequently subjected to analysis using ImageJ/Fiji.[41]

Multiple tiles were imaged to cover the entire microbial colony. These tile images were then stitched together with 10% overlap. Within each fluorescence channel, a thresholding process was applied to delineate the overall pixel area. These thresholded images were subsequently utilized for two distinct calculations: (i) determination of the total area, accomplished by applying the OR function in the Image calculator. (ii) Computation of the fused area, achieved through the application of the AND function. The total area image was used to create selection which is a demarcated area containing all pixel with intensity values. This area was then recreated on the single channel and fused images to measure pixel intensity. Using the Coloc2 plugin, a correlation was calculated for all pixels within the selected biomass area. For plotting, a subset of 10,000 random pixels was used to identify the trend in pixel intensity between the green and red channels. For quantifying the biomass area of colonies from images, the brightfield image was used. Thresholding was performed to ensure the whole biomass was included followed by area measurement in Fiji. The same brightfield images were used for convexity measurement based on pixel intensity across the biomass (plot profile) such that bright pixels indicate presence of biomass whereas dark pixels indicate background/media. These pixel intensities across the biomass were then tested for convexity along a line where a value of 0 indicates that the pixels are perfectly convex. In our case more convex is indicative of well grown biomass whereas low convexity suggests patchy/rugged growth.

Quantitative PCR-based chromosome ratio estimation

Biomass of a single spot was collected and resuspended in lysis buffer. The microfuge tubes were then heat treated (90°C for 10 minutes) to break open cells for DNA extraction. The pellet was centrifuged and supernatant diluted (1:10) for qPCR analysis. RT-qPCR was done using the iTaq Universal SYBRGreen Supermix kit (Biorad) following the vendor protocol. The reaction mix consisted of 2 μl DNA (supernatant from above), 1 μl forward primer, 1 μl reverse primer, 10 μl qPCR mastermix (contains dNTPs, enzyme and buffer), 1 μl DMSO (used for high GC DNA in Streptomyces) and 5 μl water. The primers were used at a working concentration of 0.5 uM. The target was approximately 150 bp and a range of 1 ng to 0.1 pg DNA mass was used for the standard curves. The following thermocycler program was used: 95°C for 5 min, 39 cycles of [95°C for 5s, 60°C for 30s, and 65°C for 5s], followed by 95°C for 30s.

Purified amplicons of the apramycin resistance gene (*aac(3)IV*) and hygromycin resistance gene (*hph*) were used for generating standard curves, *infB* was used as a housekeeping gene for reference. Standard curves were generated (Figure S5) for the house keeping gene (*infB*), apramycin resistance gene (*aac(3)IV*) and hygromycin resistance gene (*hph*). A serial 10-fold dilution was carried out of the pcr product followed by qPCR and plotting ct values obtained for the known copy number (Figure S5). R^2 values indicated that the Ct values can be used to accurately predict the copy number of the corresponding gene given the same PCR settings. The above slope values were used to calculate the relative proportion of apramycin and hygromycin resistance genes in samples across the antibiotic gradient. In each run purified pcr products (mentioned above) were used as reference and the sample (DNA obtained from the biomass) was the test. The following formulas were used-

$$E = 10^{(-1/\text{slope})} - 1$$

Calculation for the sample: ΔCt (test) = Ct (aac(3)IV or hph) – Ct (infB)
Calculation for the purified pcr products: ΔCt (ref) = Ct (aac(3)IV or hph) – Ct (infB)

ΔΔCt = ΔCt (test) – ΔCt (ref)

$$\text{Relative chromosome number (RCN)} = (1+E)^{-\Delta\Delta Ct}$$

Resistance and growth in antibiotic gradients

To create an antibiotic concentration gradient on the plate, filter discs were prepared with the corresponding antibiotic concentrations (50 μg/ml apramycin, 100 μg/ml hygromycin). These filter discs were then placed 1 cm from the bacterial inoculum. The layout of filter discs with different antibiotics around the inoculated spot is shown in Figure S4A. The plate was then kept in the incubator for 1 hour followed by inoculation of different strain types. After inoculation colony growth and fluorescence were tracked over time (3 to 15 days).

QUANTIFICATION AND STATISTICAL ANALYSIS

All statistical analysis was performed using R Statistical Software.[42] Significant differences and tests used have been mentioned in the results where applicable. Comparison of Mixed, Recombinant and Heterozygous strains when done in pairs was by using the Welch t test. For image analysis, pixel-wise correlation significance was calculated using Pearson's coefficient.